

<https://doi.org/10.1038/s41541-024-00811-5>

Human immunoglobulin gene allelic variation impacts germline-targeting vaccine priming

Check for updates

Allan C. deCamp^{1,16}✉, Martin M. Corcoran^{2,16}, William J. Fulp^{1,16}, Jordan R. Willis^{3,4,5}, Christopher A. Cottrell^{3,4,5}, Daniel L. V. Bader^{3,4,5}, Oleksandr Kalyuzhnyi^{3,4,5}, David J. Leggat⁶, Kristen W. Cohen¹, Ollivier Hyrien¹, Sergey Menis^{3,4,5}, Greg Finak¹, Lamar Ballweber-Fleming¹, Abhinaya Srikanth⁶, Jason R. Plyler⁶, Farhad Rahaman⁷, Angela Lombardo⁷, Vincent Philiponis⁷, Rachael E. Whaley¹, Aaron Seese¹, Joshua Brand⁶, Alexis M. Ruppel⁶, Wesley Hoyland⁶, Celia R. Mahoney¹, Alberto Cagigi⁶, Alison Taylor⁶, David M. Brown⁸, David R. Ambrozak⁶, Troy Sincomb^{3,4,5}, Tina-Marie Mullen^{3,4,5}, Janine Maenza^{1,9}, Orpheus Kolokythas¹⁰, Nadia Khati¹¹, Jeffrey Bethony¹², Mario Roederer⁶, David Diemert^{12,13}, Richard A. Koup⁶, Dagna S. Laufer⁷, Juliana M. McElrath¹, Adrian B. McDermott⁶, Gunilla B. Karlsson Hedestam²✉ & William R. Schief^{3,4,5,14,15}✉

Vaccine priming immunogens that activate germline precursors for broadly neutralizing antibodies (bnAbs) have promise for development of precision vaccines against major human pathogens. In a clinical trial of the eOD-GT8 60mer germline-targeting immunogen, higher frequencies of vaccine-induced VRC01-class bnAb-precursor B cells were observed in the high dose compared to the low dose group. Through immunoglobulin heavy chain variable (IGHV) genotyping, statistical modeling, quantification of IGHV1-2 allele usage and B cell frequencies in the naive repertoire for each trial participant, and antibody affinity analyses, we found that the difference between dose groups in VRC01-class response frequency was best explained by IGHV1-2 genotype rather than dose and was most likely due to differences in IGHV1-2 B cell frequencies for different genotypes. The results demonstrate the need to define population-level immunoglobulin allelic variations when designing germline-targeting immunogens and evaluating them in clinical trials.

Prevention of infection in licensed vaccines often correlates with the induction of protective antibodies that have sufficient breadth to cover heterogeneity among circulating strains of the target pathogen^{1–3}. Results from the Antibody Mediated Prevention (AMP) trials provide evidence that

infusion with a broadly neutralizing antibody can protect against HIV infection and support induction of bnAbs as an HIV immunization strategy^{4,5}. Germline-targeting vaccine designs are one of several approaches for generating bnAb responses to the highly variable HIV spike protein⁶.

¹Vaccine and Infectious Disease Division, Fred Hutchinson Cancer Center, Seattle, WA 98109, USA. ²Department of Microbiology, Tumor and Cell Biology, Karolinska Institutet, SE-171 77 Stockholm, Sweden. ³IAVI Neutralizing Antibody Center, The Scripps Research Institute, La Jolla, CA 92037, USA. ⁴Center for HIV/AIDS Vaccine Development, The Scripps Research Institute, La Jolla, CA 92037, USA. ⁵Department of Immunology and Microbial Science, The Scripps Research Institute, La Jolla, CA 92037, USA. ⁶Vaccine Research Center, National Institute of Allergy and Infectious Diseases, National Institutes of Health, Bethesda, MD, USA. ⁷IAVI, 125 Broad Street, 9th floor, New York, NY 10004, USA. ⁸The Foundation for the National Institutes of Health, North Bethesda, MD, USA. ⁹Department of Medicine, University of Washington, Seattle, WA 98195, USA. ¹⁰Department of Radiology, University of Washington, Seattle, WA 98195, USA. ¹¹Department of Radiology, School of Medicine and Health Sciences, The George Washington University, Washington, DC, USA. ¹²Department of Microbiology, Immunology and Tropical Medicine, School of Medicine and Health Sciences, The George Washington University, Washington, DC, USA. ¹³Department of Medicine, School of Medicine and Health Sciences, The George Washington University, Washington, DC, USA. ¹⁴The Ragon Institute of Massachusetts General Hospital, Massachusetts Institute of Technology and Harvard University, Cambridge, MA 02139, USA. ¹⁵Moderna Inc., Cambridge, MA 02139, USA. ¹⁶These authors contributed equally: Allan C. deCamp, Martin M. Corcoran, William J. Fulp. ✉e-mail: adecamp@scharp.org; gunilla.karlsson.hedestam@ki.se; schief@scripps.edu

The germline-targeting approach is based on the hypothesis that rare bnAb-precursor naive B cells with well-defined genetic signatures can be activated by a priming immunogen and subsequently matured to bnAb development by heterologous boosting. In this approach, the precursor frequency and binding affinity are critically important and depend on human genetic characteristics.

The IAVI G001 phase 1 clinical trial of eOD-GT8 60mer adjuvanted with AS01_B demonstrated that germline-targeting immunogens can induce bnAb-precursor responses in humans⁶. The vaccine was administered at weeks 0 and 8. VRC01-class immunoglobulin G (IgG) B cells were found in 35 of 36 vaccine recipients, with median frequencies among memory B cells (MBCs) reaching as high as 0.09% in the low dose group and 0.13% in the high dose group from peripheral blood mononuclear cell (PBMC) samples collected at weeks 4, 8, 10 and 16⁶. All post-vaccination MBC samples with VRC01-class B cells had higher VRC01-class frequency than at baseline for the same participant, hence all were regarded as vaccine induced. VRC01-class B cells were detected in two of twelve placebo participants, but these were detected both pre- and post-vaccination and hence were regarded as pre-existing VRC01-class memory. A dose effect was observed, with higher VRC01-class median frequencies measured in the high dose group compared to the low dose group at all MBC timepoints, including statistically significant differences at weeks 4 and 16⁶. Observation of a dose effect has potential implications for dose selection in future clinical studies and for interpreting mechanisms of germline-targeting priming immunogens. However, IAVI G001 was a placebo-controlled, double-blind, dose-escalation study investigating safety and tolerability, and as such, the two dose arms were sequentially enrolled. Therefore, dose comparisons were susceptible to confounding by unequal distributions of participant characteristics between dose groups that may impact the frequency of targeted bnAb-precursor B cells.

VRC01-class B cells are defined by utilization of an IGHV1-2 *02 or *04 heavy chain and a 5-amino acid light chain CDR3^{7–13}. In separate work, the IGHV1-2 genotype was determined with nucleotide-level precision for all trial participants in IAVI G001, by generating immunoglobulin M (IgM) libraries from each individual and applying the germline allele inference tool IgDiscover^{6,14}. In that work, use of the genotype information was limited to showing that the one participant who did not produce VRC01-class responses was the only participant lacking one of the necessary IGHV1-2 alleles (*02 or *04). Here, we looked more deeply at the genotype data, and we found an imbalance in the IGHV1-2 genotype distribution between the low and high dose groups, which suggested that the observed dose effect in VRC01-class responses might have been due at least in part to genotype differences rather than dose. We investigated whether and how the dose level and IGHV1-2 genotype affected the frequency of vaccine-induced VRC01-class IgG B cells, using statistical models tested by independent quantitative analyses of experimentally measured mRNA expression levels and B cell frequencies. We also assessed whether IGHV1-2 alleles were associated with different VRC01-class precursor affinities for the vaccine, to determine if allele effects on affinity could explain the different response rates for the two genotype-unbalanced groups.

Results

IGHV1-2 allele frequencies vary by dose group

As reported elsewhere⁶, through personalized genotyping a total of 9 different IGHV1-2 genotypes were found among the 48 IAVI G001 trial participants (Fig. 1a, b). These consisted of combinations of the known alleles *02, *04, *05 and *06, in addition to allelic variant, IGHV1-2*02_S4953, that is distinct at the nucleotide level but encodes the same amino acid sequence as the *02 allele. For the subsequent analyses in the current study, we therefore classified *02_S4953 as *02. A structural view and amino acid sequence alignment of the various IGHV1-2 alleles is shown in Supplementary Fig. 1. The frequency of each allele in the 48 trial participants showed that IGHV1-2*04 was most common, followed by IGHV1-2*02 (Fig. 1c). The one participant that did not produce a detectable VRC01-class response was found to be IGHV1-2 genotype *05/*06, i.e.

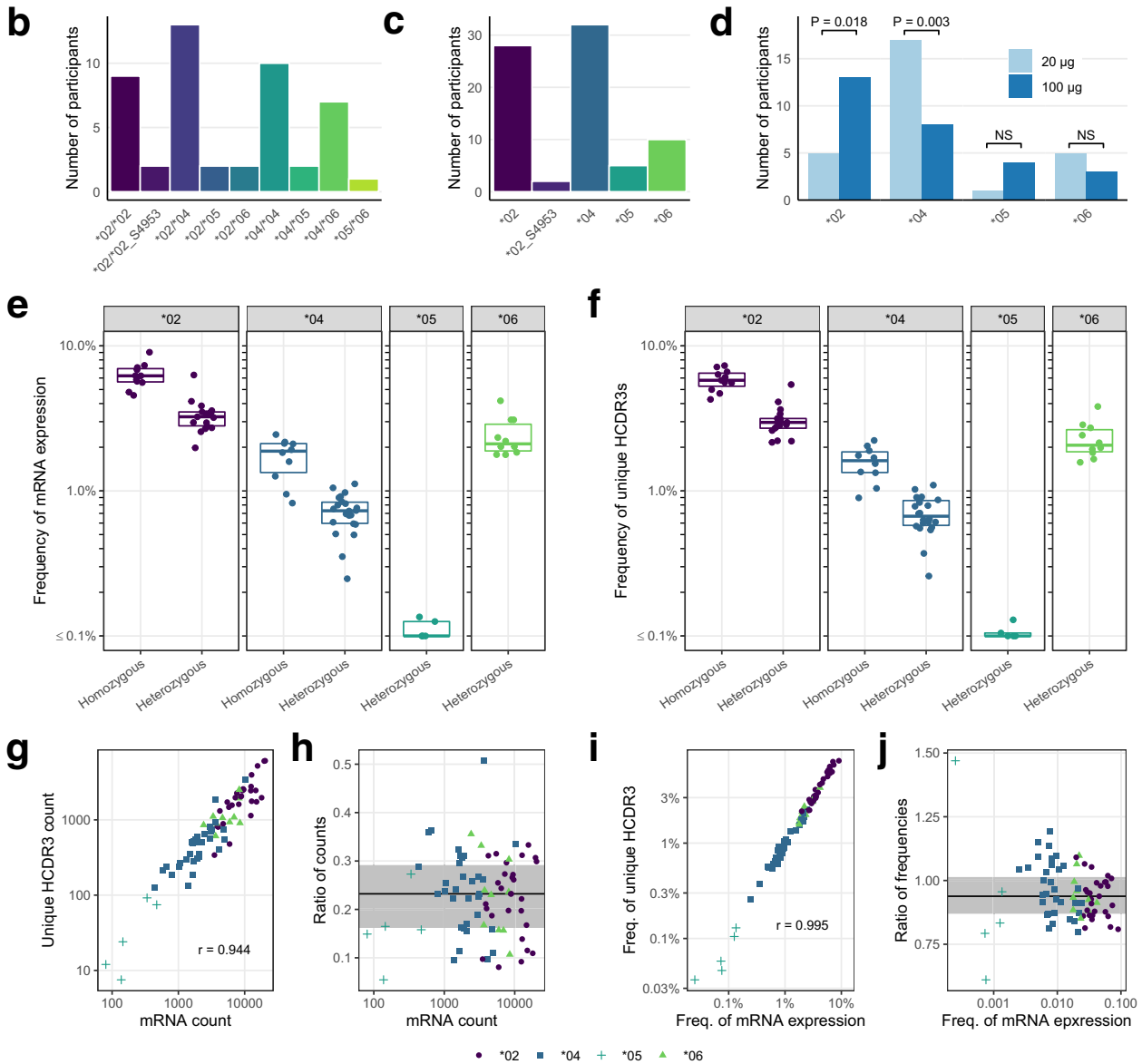
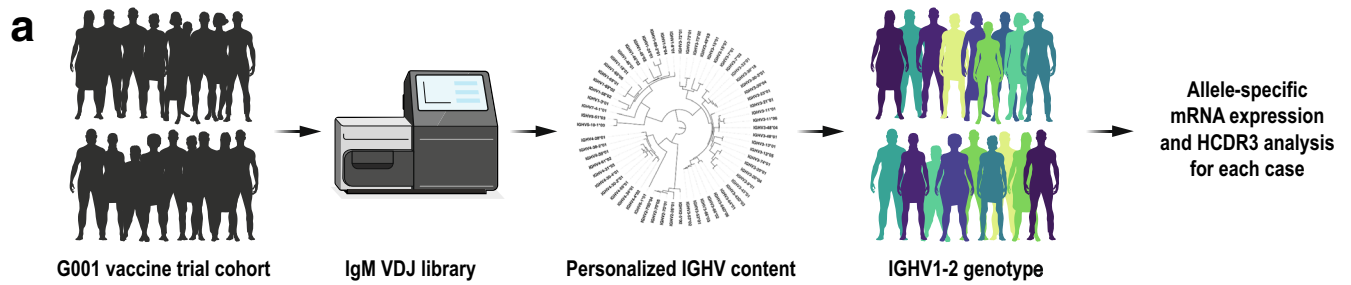
lacking one of the required *02 or *04 VRC01-class alleles, at least one of which were present in the genotype of all other trial participants (Fig. 1b and Supplementary Table 1)⁶.

We observed that the distributions of *02 and *04 alleles between dose groups were substantially uneven (Fig. 1d). In the high dose group, 72% of participants (13 of 18) had an *02 allele, compared to 28% (5 of 18) in the low dose group (P -value = 0.02). Conversely, in the low dose group, 94% of participants (17 of 18) had an *04 allele, compared to 44% (8 of 18) in the high dose group (P -value = 0.003). The *05 and *06 alleles were less prevalent and had similar frequencies between dose groups (Fig. 1d). The imbalance in *02 and *04 between dose groups potentially impacted the relative strengths of the VRC01-class responses, because a previous study had shown that the frequency of eOD-GT8-specific naive precursors in the germline repertoire was higher for individuals encoding the *02 allele compared to those encoding the *04 allele¹⁵. Therefore, we hypothesized that the dose effect observed in this trial depended on IGHV1-2 allelic differences between the groups.

IGHV1-2 allele frequencies differ in the germline repertoire

We calculated the mRNA expression frequencies of different IGHV alleles in the naive repertoire for each trial participant by counting the per-allele unique molecular identifiers (UMIs) introduced during the cDNA synthesis of IgM libraries (Fig. 1a and Supplementary Data 1). The frequencies for each IGHV1-2 allele are shown separately for homozygous and heterozygous genotypes in Fig. 1e. The mean per-allele mRNA expression of *02 was similar in homozygous and heterozygous individuals, at 3.1% (95% CI: 2.7–3.6%) and 3.3% (95% CI: 2.9–3.8%), respectively (Supplementary Table 2). Usage of *04 was ~4-fold lower, at 0.9% (95% CI: 0.7 to 1.1%) in homozygous participants and 0.7% (95% CI: 0.6 to 0.8%) in heterozygous participants (Supplementary Table 2). Comparison of the per-allele frequencies between homozygous and heterozygous participants suggested that allele usage was proportional to zygosity, with homozygotes having approximately twice the usage of *02 or *04 than heterozygotes (Fig. 1e and Supplementary Table 3). Alleles *05 and *06, which do not have the required VRC01-class binding motif, had very low usage, 0.09% (95% CI: 0.03–0.14%), and intermediate usage, 2.4% (95% CI: 1.9–3.0%), respectively (Supplementary Table 2). The differences in relative frequencies of IGHV1-2 allele usage we observed are consistent with data from two previous studies^{15,16} and from recent analysis of allele frequencies of expressed IGHV genes within a collection of previously published IgM libraries^{17,18}.

We then counted the number of unique heavy chain complementarity determining region 3 (HCDR3) sequences within IGHV1-2 mRNAs, a measure of the number of unique IGHV1-2 B cells in each personalized library (Fig. 1a and f and Supplementary Data 1). We found that, regardless of IGHV1-2 allele, the number of unique IGHV1-2 HCDR3s was proportional to the number of IGHV1-2 mRNA molecules (Fig. 1g, h), and the frequencies in the repertoire were also proportional (Fig. 1i, j). Indeed, ratios of unique HCDR3 counts to mRNA counts (Fig. 1h), a measure of 1/(B cell receptor cell surface density), were similar for *02 and *04 alleles (median 0.23 and 0.24, respectively; P -value for difference = 0.53), which suggests that the surface density was not appreciably different between these two alleles. Additionally, ratios between HCDR3 frequency and mRNA frequency for *02 and *04 (Fig. 1j) were also similar (0.93 and 0.96, respectively; P -value for difference = 0.19), which also suggested that surface density was similar in the two cases. Thus, different IGHV1-2 alleles had different frequencies of unique precursor B cells, with *02 higher than *04 (Fig. 1f). Furthermore, *02 or *04 homozygotes had approximately twice the frequency of allele-specific unique precursors as heterozygotes (Fig. 1f). Higher bnAb-precursor frequency has been shown to lead to higher bnAb-precursor-derived vaccine responses in mouse models^{19–21}. Therefore, the higher frequency of unique IGHV1-2 precursors in *02 compared to *04 individuals suggested that the stronger VRC01-class responses in the IAVI G001 high dose group could be due at least in part to the greater representation of *02 in that group. Taken together, these results supported including the *02 and *04 allele counts as independent predictors for the



frequency of vaccine-induced VRC01-class IgG B cells in our statistical models.

One model best explains the difference in VRC01-class responses between dose groups

To look for genotype-specific effects in the vaccine response data, we first analyzed differences in post-vaccination VRC01-class B cell frequencies among trial participants that were *02/*02, *02/*04, *04/*04, or *04

heterozygous with either of the non-productive *05 or *06 alleles, and we found no significant differences after adjusting for multiple comparisons (Supplementary Table 4). Similarly, we compared across dose groups with sufficient data for two genotypes: (i) *02/*04 and (ii) *04/*05 or *04/*06 (pooled genotype), and we found that neither comparison was significant (Supplementary Table 5). However, the small numbers of participants within each genotype and dose group meant that the analysis had low sensitivity. To increase sensitivity to detect genotype-specific effects, we used

Fig. 1 | IGHV1-2 genotype, allele, and pre-vaccination IgM repertoire distributions for IAVI G001 trial participants. **a** The IGHV1-2 allele content in each study participant was determined by sequencing bulk IgM libraries and inferring the IGHV allele content in each case with IgDiscover. Quantitative analyses of mRNA expression levels and HCDR3 frequencies followed. **b** Number of each genotype and **c** number of each allele, for all trial participants ($n = 48$). **d** Number of vaccine recipients per group, out of 18, with each allele (*02, *04, *05, and *06), with the *02 variant *02_S4953 classified as *02. *P*-values are based on a Fisher's exact test with values >0.05 marked as not significant (NS). For all 48 participants, pre-vaccination **e** mRNA expression frequencies and **f** unique HCDR3 frequencies for each IGHV1-2 allele are shown as points color-coded by allele and grouped by homozygous and

heterozygous genotype. Each point represents a trial participant, with heterozygous participants represented by two points. Thick lines are median values and boxes are the 25% and 75% quantiles. **g** Correlation between mRNA count and unique HCDR3 count; **h** Ratio of unique HCDR3 count to mRNA count versus mRNA count; **i** Correlation between frequency of mRNA expression and frequency of unique HCDR3s; and **j** Ratio of the unique HCDR3 frequency to the mRNA frequency versus the mRNA frequency, are shown for pre-vaccination repertoires. Points are shape- and color-coded by IGHV1-2 allele as shown in the legend of (g–j). Pearson correlation coefficients (*r*) for counts and frequencies are shown in (g and i), respectively. In panels h and j, the solid line is the median ratio, and the shaded region shows the inter-quartile range.

statistical modeling to analyze pooled data under the mechanistic assumption that allele effects were additive.

We modeled the VRC01-class response frequency using four candidate models. Each model was defined by one or more frequency parameters:

- Model 1 (Null): A single frequency for all vaccine recipients.
- Model 2 (Dose): Two frequencies, one for the low dose and another for the difference between high and low dose.
- Model 3 (Allele): Two frequencies, one each for the *02 and *04 alleles.
- Model 4 (Full): Three frequencies, one each for the *02 and *04 alleles at low dose, and another for the allele-independent difference between high and low dose.

As described in Leggat et al.⁶, for all trial participants ($n = 48$), the frequencies of VRC01-class BCRs were measured for three sample types at seven sample collection time points: (i) PBMC IgG memory B cells (MBCs) at weeks 4, 8, 10, and 16; (ii) lymph node IgG germinal center (GC) B cells at weeks 3 and 11; and (iii) PBMC IgD- plasmablasts (PBs) at week 9. Here, we modeled count data of VRC01-class BCRs using a quasi-Poisson generalized linear model. The models were fit separately for each of the seven sample collection time points and ranked based on a Quasi-likelihood criterion of Akaike's second-order information criterion (QAICc)²².

The QAICc model selection criterion ranked the models consistently at all four MBC timepoints, with the following best-to-worst order: (i) Allele; (ii) Full; (iii) Dose; and (iv) Null (Supplementary Fig. 2a and Supplementary Table 6). This model ranking indicated that the differential distributions between the dose groups of IGHV1-2 alleles *02 and *04 better explained the VRC01-class B cell frequencies post vaccination than either dose alone or a simple overall average frequency among vaccine recipients estimated by the Null model. Furthermore, the Allele model ranked higher than the Full model at all MBC timepoints, which indicated there was no detectable dose effect after accounting for the allele effect. At the week 3 GC and week 9 PB time points, the Allele model was also selected as the best model, but the ranking of the remaining models changed (Supplementary Fig. 2a and Supplementary Table 6). For the week 11 GC samples the Null model ranked highest, suggesting that neither dose nor allele adequately explained the observed variation in those samples.

Parameter estimates from the Allele model were consistently higher for the per-allele contribution of *02 to the VRC01-class response than for the contribution of *04 (Supplementary Fig. 2b and Supplementary Table 7). The Full model estimated similar per-allele effects as the Allele model but also estimated effects for high versus low dose that were close to zero and had confidence intervals that included zero in all cases (Supplementary Fig. 2b and Supplementary Table 7). Thus, the data provided no support for a true dose effect, and these results suggested that the count of *02 and *04 alleles best explained the variation in the VRC01-class B cell response to eOD-GT8 60mer.

We then compared experimentally measured VRC01-class frequencies to the Allele-model-estimated mean VRC01-class responses by genotype (Fig. 2 and Supplementary Table 8). To make comparisons in an ordered manner, we ranked IGHV1-2 genotypes based on the frequency of IGHV1-2 mRNA expression in the naive repertoire: first, we grouped genotypes that had a single *05 or *06 allele together since these alleles lack the necessary

VRC01-class motif; next, we ranked the genotypes based on our observation that *02 precursors were approximately four-fold more common than *04 precursors. This resulted in our most-to-least favorable ranking of genotypes for induction of a VRC01-class response: (i) *02/*02; (ii) *02/*04; (iii) *02/*05 or *02/*06; (iv) *04/*04; and (v) *04/*05 or *04/*06. The genotype-specific medians of the experimentally measured VRC01-class frequencies generally followed this same ordering (Fig. 2), and the model-estimated mean VRC01-class response also followed this ordering, except for the week 10 MBC timepoint where the order of *04/*04 and *02/*05 or *02/*06 was reversed (Fig. 2 and Supplementary Table 8). Hence the model captured the dependence of the VRC01-class response frequency on genotype. However, there was substantial heterogeneity in the responses that was not explained by genotype (Fig. 2). This variation was potentially attributable to other factors that can influence the strength of immune responses, including but not limited to sex, age, additional genetic factors, and immune history. Nevertheless, our modeling indicated that the effect of dose was negligible after accounting for IGHV1-2 allele content.

*02 has higher frequencies in both the naive repertoire and the modeled VRC01-class response

From the Allele model, we computed the relative contribution of *02 versus *04 alleles to the post-vaccination VRC01-class B cell frequency at each time point, and we found ratios between 1.7 and 4.4 (Fig. 3a and Supplementary Table 9). The confidence intervals in all cases included 1.0, consistent with equal contributions from *02 and *04. However, when we computed differences, rather than ratios, in post-vaccination VRC01-class B cell frequencies, we found significantly greater contributions from *02 compared to *04 (Supplementary Table 10; differences significant for all timepoints except week 10). This suggested that the true ratios were >1 . In the pre-vaccination IgM (naive) repertoire of vaccine recipients, we computed ratios for *02 versus *04 mRNA usage of 3.9 (95% CI: 3.0 to 5.3) among homozygous individuals and 4.2 (95% CI: 3.3 to 5.1) among heterozygous individuals, both of which were significantly >1.0 (*P*-values of <0.0001 and 0.0001 , respectively) (Fig. 3b and Supplementary Table 11). Ratios of the frequencies of unique HCDR3s using *02 versus *04 in the pre-vaccination repertoire were similar to the mRNA frequency ratios (Fig. 3c and Supplementary Table 11), more directly indicating higher *02 naive B cell frequencies. Overall, mRNA usage and B cell frequency were higher for *02 than for *04 in the personal naive repertoires, and *02 was higher than *04 in the Allele-model-determined contributions to vaccine-induced VRC01-class B cell frequencies.

*02 has higher frequencies among allele assignments for post-vaccination BCR sequences

Considering that VRC01-class responses from *02/*04 heterozygous individuals involved direct competition between the two alleles, we assessed frequencies of VRC01-class post-vaccination BCRs with allele assignments of *02 or *04 from *02/*04 heterozygous participants. For each VRC01-class BCR, the IGHV1-2 allele was bioinformatically assigned, accounting for the personal IGHV1-2 genotype information, as described in Leggat et al.⁶. From 873 post-vaccination BCR sequences of VRC01-class IgG (MBC or GC) or IgD- (PB) B cells from eight *02/*04 heterozygous vaccine

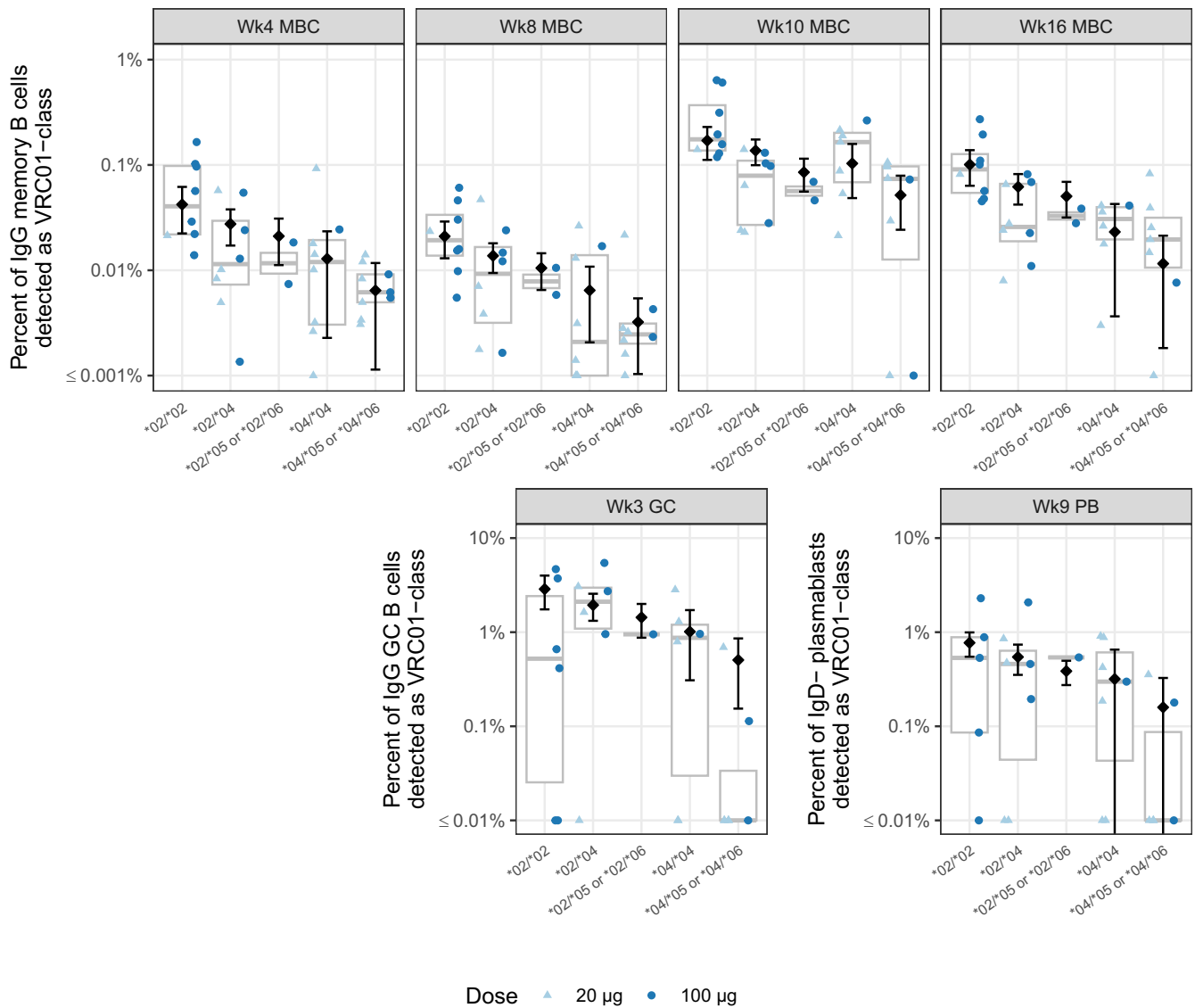


Fig. 2 | Model estimates and 95% confidence intervals (CIs) from the Allele model for each genotype and time point. Estimates and CIs for the frequency of VRC01-class IgG B cells at each time point by genotype are shown as open diamonds and vertical lines, respectively. Thick lines are median values and boxes are the 25% and 75% quantiles. Experimentally measured frequencies for each participant are shown

as color- and shape-coded points by dose group as indicated by the legend. Genotypes containing the *05 and *06 alleles are grouped together (e.g., *02/*05 or *02/*06), because the estimated mean response from the Allele model depends only on the count of *02 and *04 alleles. Week 11 germinal center (GC) results are not shown since the Null model ranked higher than the Allele model for that sample time point.

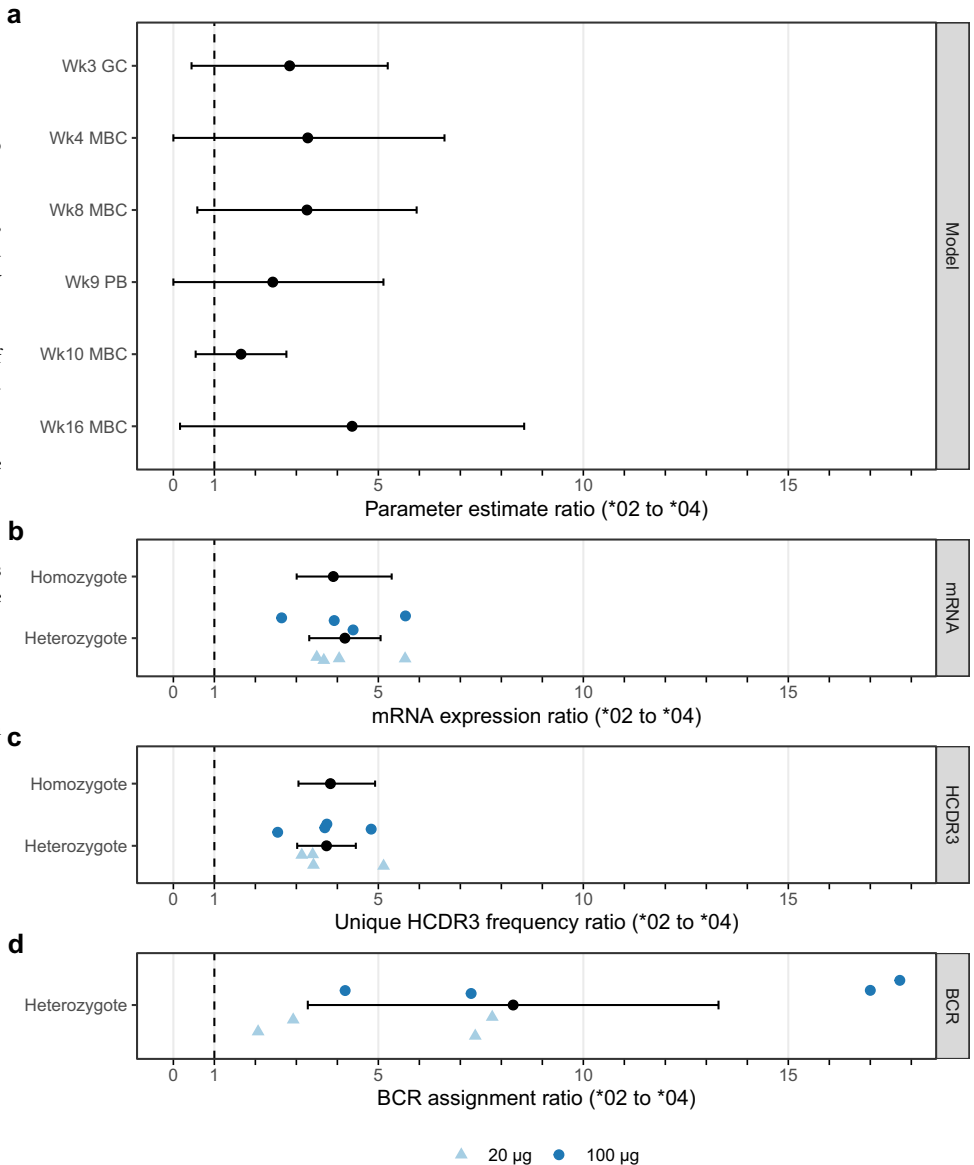
recipients, we computed the per-participant ratio of *02 to *04 as the assigned germline allele (Fig. 3d and Supplementary Table 12). Only four of 873 (0.46%) BCR assignments were ambiguous, hence allele ambiguity did not meaningfully affect our calculations. The overall median ratio of *02 to *04 was 7.3 (range, 2 to 17.7) (Supplementary Table 12), which was significantly >1.0 (P -value = 0.004). The ratio of *02 to *04 BCRs varied widely (0 to infinity) across different post-vaccination time points but was >1.0 in 89% (42/47) of cases (Supplementary Table 13). The observed BCR usage ratios (Fig. 3d and Supplementary Tables 12–13) were generally higher than the model-derived usage ratios (Fig. 3a and Supplementary Table 9) and the naive repertoire mRNA and HCDR3 frequency ratios (Fig. 3b, c and Supplementary Table 11). We tested for a dose effect in the data in Fig. 3d but found no significant effect (P -value = 0.154). IGHV1-2*02 differs from *04 by a single nucleotide (A^{*04}/T^{*02}, SNP rs112806369) and a single amino acid (Arg₆₆^{*04}/Trp₆₆^{*02}, Kabat residue numbering) (10,15,23). We documented several occurrences of the Arg₆₆^{*04}→Trp₆₆^{*02} mutation, which is favorable for VRC01-class maturation, in post-vaccination VRC01-class BCRs from *04 homozygous individuals⁶. Thus, occurrence of this mutation might

have inflated the *02 to *04 germline allele ratio in BCRs of heterozygous individuals shown in Fig. 3d. Overall, the *02 to *04 ratios among BCRs from heterozygotes were consistent with the conclusions of the Allele model in that both indicated stronger VRC01-class responses from the *02 allele. Those findings, combined with the fact that the naive repertoire mRNA and HCDR3 ratios demonstrated higher expression and B cell frequency for the *02 allele, suggested a simple potential explanation for the superiority of *02 over *04 for VRC01-class responses, namely that the higher frequency of *02-using B cell precursors translated into higher post-vaccination VRC01-class responses.

Naive repertoire predicts outcome

To test the hypothesis that stronger VRC01-class responses resulted from higher B cell precursor frequencies, we looked for correlations between the VRC01-class response and the total frequency of IGHV1-2*02 or *04 B cells in the naive repertoire. Pooling across dose groups (Fig. 4), we found significant correlations at each time point, excluding week 11, with correlation coefficients ranging from 0.4 to 0.6 (Fig. 4, P -values ranging from 0.04 to

Fig. 3 | Relative contribution of *02 versus *04 alleles to Allele-model-derived post-vaccination VRC01-class frequency, pre-vaccination IGHV1-2 mRNA expression level, and post-vaccination BCR assignments. **a** Allele model estimates for the relative contribution of *02 versus *04 (as a ratio) to the post-vaccination VRC01-class frequency are shown with 95% confidence intervals (CIs) for germinal center (GC) B cell, memory B cell (MBC), and plasmablast (PB) samples taken at the indicated week (Wk) after first vaccination. **b** Experimentally measured pre-vaccination ratios of *02 to *04 mRNA expression levels for homozygous or heterozygous genotypes. For homozygotes, the ratio of means and CI for *02 and *04 individuals is shown. For heterozygotes, ratios for each individual are shape- and color-coded ($N = 4$ for low dose; $N = 4$ for high dose), and the overall mean ratio and CI are shown in black. **c** Experimentally measured pre-vaccination ratios of *02 to *04 unique HCDR3 frequencies for homozygous or heterozygous genotypes. Homo- and heterozygote data are displayed as in (b). **d** Ratio of *02 to *04 usage for germline allele assignments among post-vaccination BCRs recovered from eight vaccine recipients known to be heterozygous for *02 and *04 by pre-vaccination genotyping are shape- and color-coded ($N = 4$ for low dose; $N = 4$ for high dose), and the overall mean ratio and CI are shown in black.



0.0003). Analyzing dose groups separately, both dose groups showed positive correlations at MBC timepoints, but the correlations were stronger and statistically significant only for the high dose group. At GC timepoints, we found significant positive correlations only in the low dose group (Supplementary Fig. 3). The difference in correlation strength could reflect a dose effect but could also be explained by the fact that the high dose group, which was over-represented by *02, generally had stronger VRC01-class responses with higher dynamic range and had higher standard deviation of HCDR3 frequency perhaps due to its wider range of genotypes. Whatever the explanation, the significant positive correlations in the pooled data demonstrated that the strength of the VRC01-class response increased monotonically with the total frequency of IGHV1-2*02 and *04 naive precursors. This finding, together with the observation that the experimentally measured naive precursor frequency was higher for *02 than for *04, indicated that the stronger VRC01-class responses for *02 were most likely due simply to higher naive B cell frequencies for *02. Thus, experimental data provided independent corroboration for our statistical modeling.

Alleles affect precursor affinities

The fundamental hypothesis of the germline-targeting priming strategy is that vaccine antigen affinity and avidity for rare bnAb-precursor B cells

strongly impacts whether or not the vaccine can trigger GC and memory responses from those precursors. Hence, while our above analyses focused on precursor frequency, it was also important to consider whether affinity differences between alleles could explain the different response outcomes. To begin, we investigated the effect of the IGHV1-2 *05 and *06 alleles on the affinity of eOD-GT8 for VRC01-class precursors. Alleles *05 and *06 both possess Arg⁵⁰ instead of Trp⁵⁰, one of the critical VRC01-class germline residues that interacts with HIV gp120. We produced W50R variants of VRC01-class precursors that were originally *02 or *04, including inferred germline (iGL) precursors for two bnAbs (VRC01 and N6), iGLs for four post-vaccination BCRs in the IAVI G001 low dose group⁶, and four human naive precursors isolated by prior B cell sorting studies of HIV-unexposed individuals^{24,25}. We then assessed eOD-GT8 binding affinity for the original and W50R-variant iGL precursors using surface plasmon resonance (SPR). The original precursors all bound to eOD-GT8, with a median KD of 120 nM, whereas only one of the W50R variants had detectable affinity, and the overall median KD was $\geq 100 \mu\text{M}$ (Fig. 5a and Supplementary Data 2). The only W50R binder (KD, 4.0 μM) derived from the highest affinity original Ab, VRC01 iGL (KD, 49 pM), with an ~80,000-fold loss in affinity due to W50R. These results provided an explanation for why eOD-GT8 60mer failed to induce VRC01-class responses in the one *05/*06 participant.

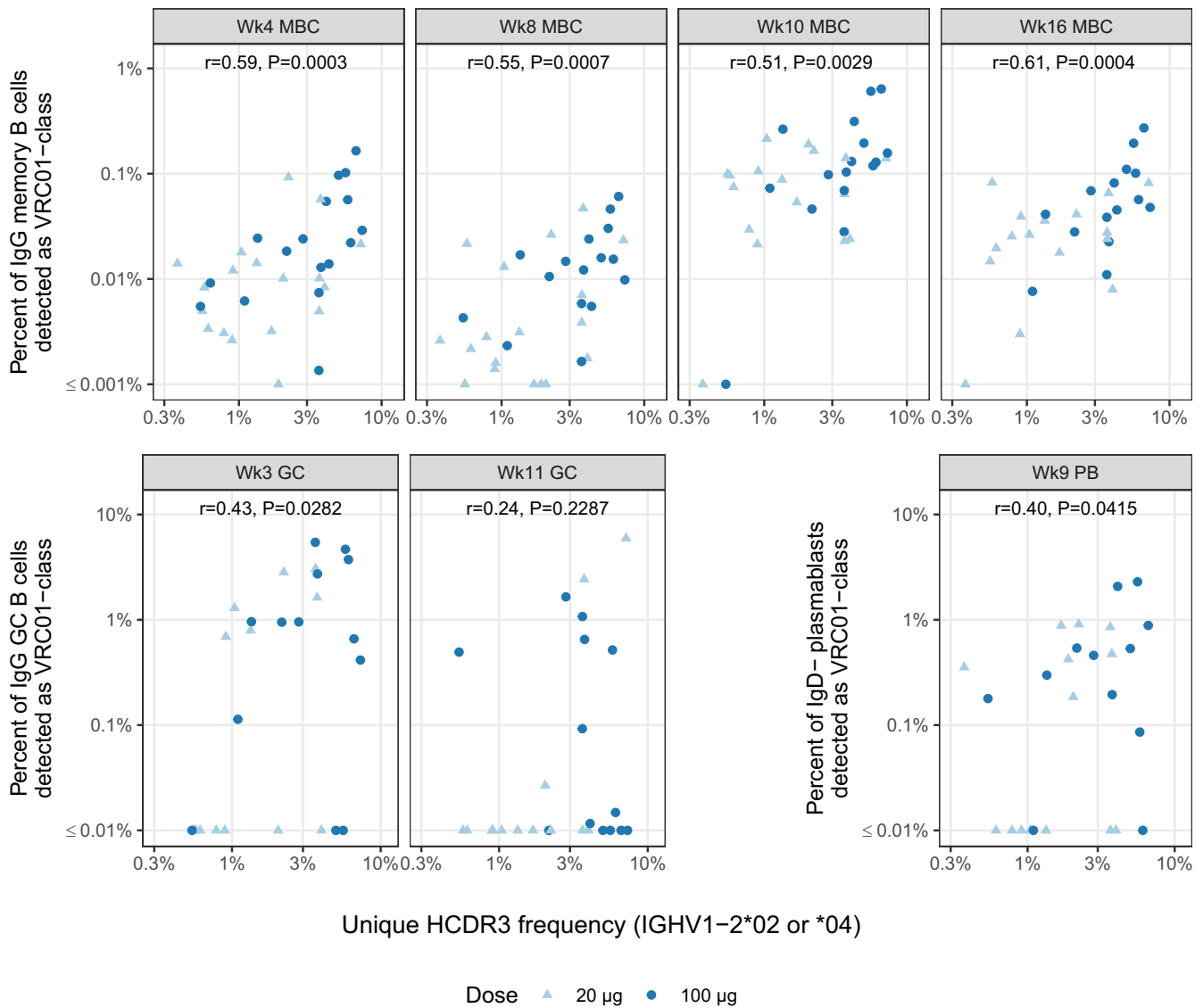
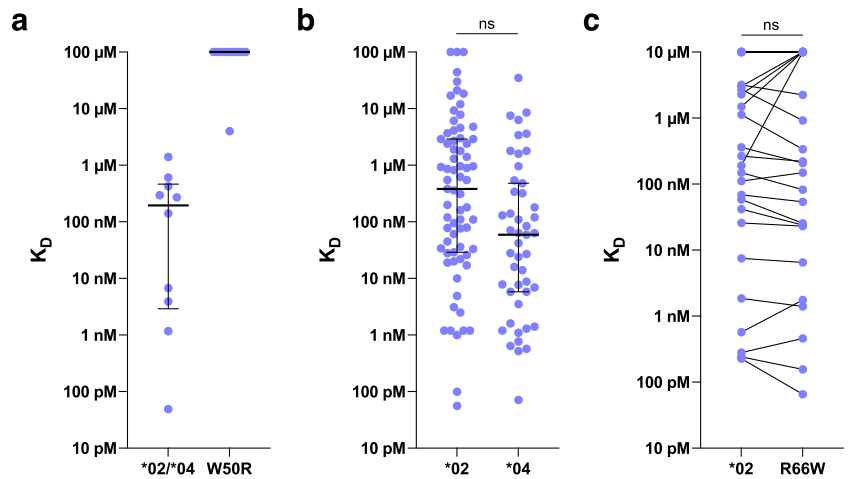


Fig. 4 | Correlations between pre-vaccination IgM unique HCDR3 frequency (IGHV1-2*02 or *04) and the percent VRC01-class B cell response by visit. Points are shape- and color-coded as shown in the legend. Spearman correlation coefficient (r) and P-values are displayed for each time point.

Fig. 5 | Affinity analyses of VRC01-class IGHV1-2 allele variants. a Affinities of VRC01-class precursors from two bnAb iGLs, four human naive precursors, and four iGLs from week 3 post-vaccination BCRs from IAVI G001, with original *02 or *04 Abs on the left, and W50R variants of those Abs on the right. **b** Affinities of *02 (N = 71) and *04 (N = 47) iGLs from post-vaccination BCRs from IAVI G001. **c** Affinities of *02 VRC01-class iGL antibodies from IAVI G001 and for *04 (R66W) variants of the same antibodies (N = 28 each). Lines connect matched Ab variants. In (a, b), horizontal lines indicate median and interquartile range. In (a-c), all affinities were measured for eOD-GT8 monomer analyte, and all iGLs from IAVI G001 are from the low dose group.



To complement our findings above that VRC01-class *02 precursors had higher frequencies than *04 in IAVI G001, we evaluated whether the two precursor populations had differing affinities for eOD-GT8. We first re-analyzed the Leggat et al. data on eOD-GT8 affinities for inferred germline (iGL) variants of post-vaccination VRC01-class BCRs recovered from the low dose group. These iGLs were overwhelmingly (96%) derived from memory BCRs after the first or second vaccination, hence they represented precursors to vaccine responses that survived GC competition and became memory B cells in the blood. Leggat et al. reported statistics on all VRC01-class iGLs (median K_D , 119 nM; $N = 118$), but here we examined the data for *02 and *04 iGL precursors separately. We found that *04 iGLs, with median K_D of 59 nM and interquartile range of 5.8 nM to 480 nM ($N = 47$), had approximately six-fold higher affinities than *02 iGLs (median K_D , 380 nM; interquartile range, 29 nM to 2.9 μ M; $N = 71$) (Fig. 5b and Supplementary Data S2). However, using a repeated measures test to account for the fact that affinities for different antibodies from the same participant are potentially correlated (the $N = 47$ *04 Abs came from 14 participants, and the $N = 71$ *02 Abs came from 5 participants), the six-fold difference was not significant (p -value, 0.38). Furthermore, we tested directly whether *04 precursors had inherently higher affinity than *02 precursors as a consequence of the R66W mutation that distinguishes *02 (Arg⁶⁶) from *04 (Trp⁶⁶). Although this mutation is not located within the region of direct antibody-antigen contacts, the spatial location of this mutation suggested that an indirect (allosteric) effect on affinity was possible (Supplementary Fig. 1). To test for such an effect, we produced 28 different *02 VRC01-class iGL antibodies from the IAVI G001 low dose group, along with *04 (R66W) variants of the same antibodies, and we measured their affinities for eOD-GT8 monomer by SPR (Fig. 5c and Supplementary Data 2). We found that the original *02 iGLs (median K_D , 310 nM; interquartile range, 30 nM–8.3 μ M; $N = 28$) had indistinguishable affinities to their *04 variants (median K_D , 280 nM; interquartile range, 23 nM–10 μ M; $N = 28$; repeated measures test p -value, 0.64). We concluded that neither allele had a precursor affinity advantage over the other. Therefore, affinity differences between alleles could not explain the different response outcomes between the vaccine groups.

Discussion

The IAVI G001 clinical trial established proof of concept for the germline-targeting strategy of priming bnAb-precursor B cell responses⁶. In this study we extend those results to show how Ig genotype influenced the human response to the vaccine used in the trial. Higher frequency VRC01-class responses were observed in the high dose compared to the low dose group, but here, through quantification of personalized allele usage, HCDR3 frequencies, and allele-specific mAb affinities, and statistical analyses of genotype effects, we have demonstrated that the apparent dose effect is best explained by an imbalance in IGHV1-2 alleles between dose groups. The results of this study, while not precluding that there could be a true dose effect within genotype, show that functionally consequential allelic variation can impact the performance of germline-targeting vaccine priming on at least two levels. First, particular germline alleles can dramatically alter affinity for the priming immunogen and thereby act as an on-off switch for the desired response, as demonstrated by the >4-orders of magnitude loss of eOD-GT8 affinity for precursors with the W50R mutation present in the *05 and *06 alleles, and the corresponding absence of VRC01-class responses in the *05/*06 heterozygous genotype participant in contrast to all other participants. Second, different alleles can have different utilization frequencies within the naive repertoire, and corresponding different B cell frequencies, which can translate directly into different vaccine response frequencies, as demonstrated here by the highest responses being consistently found in cases that contained at least one *02 allele compared to those that did not have any *02 allele.

Our study supports the idea that germline-targeting approaches in general should consider both the affinity effects and the relative abundances of the targeted alleles in the naive repertoire, both of which are dependent on the genotype. Furthermore, imbalances across groups in the allele

distributions of the targeted bnAb-precursor in a trial of a germline-targeting vaccine should be accounted for when making group comparisons. For clinical tests of germline-targeting immunogens, our results encourage a practice of genotyping of trial participants for antibody genes relevant to the antibody-antigen interaction in question. The genotype information should be used either during randomization into groups, to ensure a balanced distribution of relevant alleles in advance, or during analysis of trial results in concert with statistical modeling, mRNA usage quantification, and antibody affinity analysis approaches described here, to ensure that allele-specific effects can be controlled. Overall, our results emphasize the importance of accounting for allele content and the frequencies of these alleles in the naive repertoire when developing and analyzing germline-targeting vaccines.

Our results also provided evidence that precursor frequency affects the ability of germline-targeting priming immunogens to induce bnAb-precursor-derived responses in humans. In mouse models, it has been established that the performance of a germline-targeting immunogen depends on at least three factors: (1) the target precursor B cell frequency, (2) the monovalent affinity of the precursor B cell to the immunogen, and (3) the avidity or multivalency of the immunogen^{7,19–21,24,26}. The eOD-GT8 60mer immunogen was designed to achieve high affinity and avidity (criteria 2 and 3) for diverse VRC01-class precursors, with the assumption that targeting diverse precursors would increase the target precursor B cell frequency (criteria 1) and would be needed to target a sufficiently large pool of precursors in any individual at any one time. Human genetic diversity and antibody recombinational diversity underlie the assumed need to target diverse precursors sharing a minimal required set of bnAb characteristics^{23,24,27}. We found that the frequency of IGHV1-2*02 mRNA usage was approximately four-fold higher than for the *04 allele, and correspondingly, we found that the *02 naive B cell frequency was approximately four-fold higher than for the *04 allele, consistent with a previous observation of higher frequencies of eOD-GT8-specific VRC01-class precursors in *02 compared to *04 individuals¹⁵. We also showed that neither allele had an affinity advantage. Thus, increased precursor frequencies in *02 individuals provide a simple potential mechanistic explanation for the elevated post-vaccination VRC01-class frequencies we observed here in *02 compared to *04 participants. Taken together, these results provide evidence that bnAb precursor frequency (criterion 1) is also important in humans, and that individual-to-individual variation in VRC01-class precursor frequency was controlled by IGHV1-2 genotype variation in this trial.

Our findings underscored the utility of statistical modeling for identifying mechanistic effects in clinical data. The IAVI G001 clinical study was not originally designed to study genotype-specific effects, and consequently, comparisons between VRC01-class responses for different genotypes at any one time point were not sufficiently powered to detect differences. However, in our models we used the simplifying assumption that each allele contributes to the VRC01-class response independently, which allowed us to estimate *02 and *04 allelic effects using data from nearly all vaccine recipients. At most time points, we found that *02 and *04 allele content alone best predicted the VRC01-class response; that is, allelic content predicted the vaccine-induced response better than dose, and after adjusting for allelic content, dose did not sufficiently explain the remaining variation in the vaccine-induced response to warrant inclusion in the best model. We therefore established that trial participant IGHV1-2 allele content confounded the relationship between dose and the vaccine response. We believe this is the only known example of an established confounder of the dose effect found in a clinical dose-escalation vaccine trial. A Pubmed search using the search terms “confound”, “vaccine”, and “dose escalation” resulted in two references^{28,29}, neither of which discussed confounding of dose with a baseline participant characteristic.

These results add to a growing body of work investigating the importance of germline variation in immunoglobulin genes and the role of this variation in antibody response to various targets. Early studies of allele effects on antibodies against *Haemophilus influenzae* type b (Hib) dependent on either IGHV3-23 or IGK2-29 revealed geographic and ethnic population-dependent variations in polymorphisms that can affect

antibody affinity or expression levels, and also showed that copy number variations that could affect expression levels^{30–33}. The structural interaction of anti-influenza IGHV1-69 bnAbs with the Hemagglutinin stem depends in part on Phe^{543–57}, a residue encoded in most but not all VH1-69 alleles, with other alleles having Leu^{543,38}. Polymorphism at IGHV1-69 position 54 has been shown to impact responses to the influenza hemagglutinin stem epitope during infection or vaccination, with higher germline affinities usually but not always associated with Leu^{543,38,39}, and stronger memory B cell responses and serum antibody binding responses occurring for Phe⁵⁴ homozygotes than Leu⁵⁴ homozygotes, potentially due to preferred IGHV1-69 germline gene usage for Phe⁵⁴ alleles^{38–40}. Different classes of HIV bnAbs derive from different antibody genes⁴¹, and the allelic dependencies in most cases remain to be elucidated. The considerations and methods employed in our study should assist further exploration of genotype effects on antibody immunity.

Our results suggest that the lower dose could be used in future studies of eOD-GT8 60mer/AS01_B, based on: (i) our analyses showing lack of a true dose effect; (ii) the separate demonstration of favorable affinity maturation of VRC01-class compared to non-VRC01-class BCRs studied for the low dose group⁶, which in light of our present analysis shows that the low dose responses were highly productive even in cases with a genotype disadvantage; and (iii) the general consideration that the lowest safe and effective dose should be used. Furthermore, given that germline-targeting priming immunogens are designed with the intention of providing a competitive advantage to bnAb-precursor B cells, intuitively one would expect that reducing the dose might improve performance by retaining bnAb-precursor activation while reducing non-specific activation of competitors.

Despite the fact that VRC01-class responses were weaker in *04 compared to *02 individuals, we note that VRC01-class response rates and frequencies were nevertheless high among *04 homozygous individuals (e.g., 100% positivity and median frequency of 0.16% among MBCs at week 10; $N = 7$) and even among *04/*05 or *04/*06 heterozygous individuals (e.g. 88% positivity and median frequency of 0.07% at wk 10; $N = 8$)⁶. Thus, the vaccine was able to induce strong VRC01-class IgG B cell responses regardless of IGHV-1 genotype, for individuals with at least one required allele (*02 or *04). Given that ~90% of humans are at least heterozygous for *02 or *04¹⁵, our analyses of the IAVI G001 trial provide further encouragement for attempts to develop a vaccine to induce VRC01-class bnAbs. The implications of this study are not limited to IGHV1-2, however. Germline-targeting vaccines targeting other bnAbs for HIV or other pathogens will depend on other human antibody gene variants. This study illustrates for the first time how immunoglobulin genotype can modulate human vaccine responses and how personalized immunoglobulin genotyping can be employed to control for and potentially predict such effects.

Methods

Study design

IAVI G001, with ClinicalTrials.gov registry number NCT03547245, was a phase 1, randomized, double-blind, placebo-controlled dosage escalation study to evaluate the safety and immunogenicity of eOD-GT8 60mer vaccine adjuvanted with AS01_B in HIV-uninfected, healthy adult volunteers. All participants in the trial provided written informed consent⁶. Additional details are in Leggat et al.⁶. Here, we employed immunoglobulin heavy chain variable (IGHV) genotyping, statistical modeling of VRC01-class vaccine responses, quantification of IGHV1-2 allele usage and B cell frequencies in the naive repertoire for each trial participant, and SPR analyses of antibody affinities to investigate a potential genetic explanation for the observed stronger VRC01-class responses in the high dose group of the trial. We assessed the dependence of post-vaccination VRC01-class B cell frequencies on IGVH1-2 genotype alone, dose alone, or genotype and dose, and on pre-vaccination naive repertoire IGVH1-2 allele mRNA expression frequencies and unique precursor B cell frequencies. Additionally, we assessed *in vivo* competition between IGHV1-2 alleles by evaluating post-vaccination BCR IGHV1-2 gene assignments in VRC01-class responses.

Ethics statement

The trial was conducted under an Investigational New Drug (IND) application submitted to the US Food and Drug Administration and carried out in compliance with the protocol filed within the IND as described in Leggat et al.⁶. IGHV genotyping of the G001 participants was performed under an ethics approval from the National Ethical Review Agency of Sweden (decision no. 2021-01850), as described in Leggat et al.⁶.

B cell sorting and sequencing and inferred germline analysis

The primary immunogenicity readout in the trial, frequency of VRC01-class IgG B cells, was measured by fluorescence-activated cell sorting (FACS) and single B cell sorting, B cell receptor sequencing, and bioinformatic analysis, as described in Leggat et al.⁶.

Next generation sequencing (NGS) library preparation

The procedures described in Leggat et al.⁶ and Vazquez Bernat et al.⁴² were utilized in NGS library preparation. In brief, following cDNA synthesis with an IgM-specific primer that contained a Unique Molecular Identifier (UMI) and a universal amplification sequence, two independent IgM libraries were prepared for each trial participant ($N = 48$). The first utilized a 5' multiplex primer set that targets all functional IGHV leader regions (leader library) and the second a 5' multiplex set that targets the 5' untranslated region (UTR) of the same genes (5'UTR library). In both cases the universal reverse primer was used as the reverse primer. All primer sequences are described in Supplementary Data S3.

Genotype analysis and relative IGHV mRNA quantification

The amplified libraries were individually indexed and sequenced using the Illumina MiSeq platform version 3 (2 × 300 cycle) kit to enable full VDJ coverage. The merged read numbers for the two independent IgM libraries produced for each of the 48 cases are shown in Supplementary Data S4. The merged IgM library size ranged from 488,061 to 1,693,395 reads, with an average of 929,106 merged reads for each case. IGHV germline inference using IgDiscover (version v1.0.1 (2022-11-16)) was performed to identify the genotype of each case, as described in⁴² using the default parameters and the IMGT human IGH database, downloaded in April 2021, as a starting reference database. The full set of 96 IgM libraries were also analyzed using the AIRR reference human database, <https://ogrdp.airr-community.org/>, and individually genotyped using the *corecount* genotyping software⁴³ with the vast majority of the IGHV genes captured in each of the cases analyzed (Supplementary Fig. 4), except genes that are known to be deleted in some individuals and genes that are very infrequently used in IgM repertoires (the six genes at the bottom of the plot). In addition to producing an individualized genotype for each case, the output of the program provided a count of the number of unique UMIs associated with sequences with zero differences from the inferred individualized germline set. This enabled the UMI count of unmutated sequences to be utilized as a means of calculating overall frequency of unmutated germline alleles in the mRNA molecules used to produce the library. The number of unique UMIs associated per allele of the individualized genotype was used to calculate the overall frequency of different IGHV alleles in the full naive repertoire in the 5'UTR libraries and the leader libraries of each case in this study and to calculate the relative frequency of different alleles of the IGHV1-2 gene.

IGHV1-2 HCDR3 frequency quantification

The IgDiscover program determined the number of unique HCDR3s present in the full germline set of UMI containing unmutated IGHV allelic sequences. This enabled the calculation of the frequency of unique HCDR3s associated with each IGHV germline allele present in the 5'UTR IgM libraries and the IgM leader libraries of each case.

IGHV1-2 allele usage analysis

For each participant allele, the relative usage for that allele was the mean frequency of the two primer sets. For two participants with

*02/*02_S4953 genotype, we reported allele usage for *02 as the sum of the mean frequencies from the two primer sets for the *02 and *02_S4953 alleles. As noted in Leggat et al.⁶, the *02_S4953 allele is a variant of *02 with a non-coding polymorphism and a similar relative frequency as the *02 allele.

Statistical modeling analysis

The goal of the statistical modeling analysis is to identify whether and how the effect of dose and/or IGHV1-2 genotype allele composition predict the VRC01-class B cell response at post-vaccination time points. At each of the seven sample collection time points, the frequency of VRC01-class IgG B cells was estimated by taking the product of the frequency of epitope-specific IgG B cells measured using FACS and the frequency of VRC01-class IgG B cells among successfully sequenced epitope-specific B cells measured by B cell sorting, sequencing and bioinformatic analysis, as described in Leggat et al.⁶. We estimated the total number of VRC01-class IgG B cells (V) in each sample by taking the frequency estimate and multiplying by the number of VRC01-class IgG B cells rounded to the nearest integer. We modeled the count data V along with the total number of IgG B cells (N) using an over-dispersed Poisson (or quasi-Poisson) distribution, a relaxed Poisson distribution that allows for the variance to be greater than the mean⁴⁴. Estimation was performed using the method of quasi-likelihood⁴⁵. We defined four models (Null, Dose, Allele, and Full) for each time point given an expectation formula describing the relationship between V and N and the following participant level covariates:

$$\mathbb{I}_{Dose=100\mu g}$$
 an indicator of being in the high dose group (1)

$$n02$$
 the IGHV1-2*02 zygosity (0, 1 or 2) (2)

$$n04$$
 the IGHV1-2*04 zygosity(0, 1, or 2) (3)

where the four expectation formulas (identified by the name in parentheses) are:

$$(Null) E(V|N) = \beta_{Intercept} \cdot N$$
 (4)

$$(Dose)E(V|Dose, N) = \beta_{Dose=20\mu g} \cdot N + \beta_{Dose\ delta(100\mu g-20\mu g)} \cdot \mathbb{I}_{Dose=100\mu g} \cdot N$$
 (5)

$$(Allele)E(V|n02, n04, N) = \beta_{*02} \cdot n02 \cdot N + \beta_{*04} \cdot n04 \cdot N$$
 (6)

$$(Full) \beta_{*02} \cdot n02 \cdot N + \beta_{*04} \cdot n04 \cdot N + \beta_{Dose\ delta(100\mu g-20\mu g)} \cdot \mathbb{I}_{Dose=100\mu g} \cdot N$$
 (7)

Each model was defined by one or more betas that defined a population average frequency of VRC01-class response among a group of vaccine recipients (Table 1). Figures that show these beta estimates use are annotated using the subscript.

Table 1 | Interpretation of model coefficients

Model(s)	Beta	Interpretation
Null	$\beta_{Intercept}$	Overall vaccine-induced mean response pooling over dose groups
Dose	$\beta_{Dose=20\mu g}$	Mean response in the low dose group
Dose, Full	$\beta_{Dose\ delta(100\mu g-20\mu g)}$	Difference in mean response between dose groups
Allele, Full	β_{*02}	Mean IGHV1-2*02 per-allele response
Allele, Full	β_{*04}	Mean IGHV1-2*04 per-allele response

At each time point these models were ranked using the Quasi-likelihood version of Akaike’s second-order information criterion (QAICc)²².

Bioinformatic B cell receptor (BCR) sequence analysis

BCR allele assignments were made with the adaptive immune receptor repertoire (AIRR) module within the Sequencing Analysis and Data library for Immunoinformatics Exploration (SADIE) library (<https://github.com/jwillis0720/sadie>). The SADIE AIRR module ports IgBLAST⁴⁶ for analysis of nucleotide sequences and ensures that the data are represented in AIRR recombination schema that defines a data model, field names, data types, and encodings⁴⁷. SADIE AIRR provides the user with scriptable, granular control over IgBLAST options via a python API or a command-line interface. SADIE AIRR determined optimized V(D)J alignment penalties to find a productive recombination (adaptable penalty model) and corrected insertions and deletions that were absent in the germline alignment produced by IgBLAST v1.17.1. The final allele call was based on the lowest e-value. An allele was ranked “ambiguous” if there were two or more alleles with the same e-value. That is, the mature sequence was 1 nucleotide away from two or more germline alleles. BCRs ambiguous for *02/*04 are equiprobable for each allele therefore were assigned a count of 0.5 for each allele.

Antibody production for SPR

Genes encoding the antibody Fv regions were synthesized by GenScript and cloned into antibody expression vectors pCW-CH1g-hG1, pCW-CL1g-hL2, and pCW-CL1g-hk. Monoclonal antibody production was conducted in house using transient transfection of HEK-293F cells (ThermoFisher) and purification using rProtein A Sepharose Fast Flow resin (Cytiva).

Antigen production for SPR

His-tagged and avi-tagged monomeric eOD-GT8 was produced by transient transfection of HEK-293F cells (ThermoFisher) and purified by immobilized metal ion affinity chromatography (IMAC) using HisTrap excel columns (Cytiva) followed by size-exclusion chromatography (SEC) using Superdex 75 10/300 GL (Cytiva).

SPR

The data in Fig. 5b was measured in Leggat et al.⁶, while the data in Fig. 5a, c were measured in this work. In all cases, we measured the kinetics and affinities of antibody-antigen interactions on a Carterra LSA instrument using HC30M or CMDP sensor chips (Carterra) and 1x HBS-EP+ pH 7.4 running buffer (20x stock from Teknova, Cat. No H8022) supplemented with BSA at 1 mg/ml. We followed Carterra software instructions to prepare chip surfaces for ligand capture. In a typical experiment, ~2500–2700 RU of capture antibody (SouthernBiotech catalog # 2047-01) in 10 mM Sodium Acetate pH 4.5 was amine coupled. The critical detail here was the concentration range of the amine coupling reagents and capture antibody. We used N-Hydroxysuccinimide (NHS) and 1-Ethyl-3-(3-dimethylamino-propyl) carbodiimidehydrochloride (EDC) from Amine Coupling Kit (GE order code BR-1000-50). As per kit instruction 22-0510-62 AG, the NHS and EDC should be reconstituted in 10 ml of water each to give 11.5 mg/ml and 75 mg/ml respectively. However, the highest coupling levels of capture antibody were achieved by using 10 times diluted NHS and EDC during surface preparation runs. Thus, in our runs the concentrations of NHS and EDC were 1.15 mg/ml and 7.5 mg/ml. The concentrated stocks of NHS and EDC could be stored frozen in -20C for up to 2 months without noticeable loss of activity. The SouthernBiotech capture antibody was buffer exchanged into 10 mM Sodium Acetate pH 4.5 using Zeba spin desalting columns 7 K MWCO 0.5 ml (catalog # 89883 from Thermo) and was used at concentration 0.25 mg/ml with 20 min contact time. Phosphoric Acid 1.7% was our regeneration solution with 60 s contact time and injected three times per each cycle. Solution concentration of ligands was around 5 ug/ml and contact time was 3 min. Raw sensograms were analyzed using Kinetics software (Carterra), interspot and blank double referencing, Langmuir

model. Analyte concentrations were quantified on NanoDrop 2000c Spectrophotometer using absorption signal at 280 nm. A typical SPR run tested 6 different analyte concentrations using a dilution factor of 4. Maximum analyte concentration for eOD-GT8 was 87 μ M for Fig. 5a and 10 μ M for Fig. 5c. For the data from Leggat et al.⁶ in Fig. 5b, maximum analyte concentration was generally 10 μ M, except for weak binders which were generally re-run at higher maximum analyte concentrations of 50 or 118 μ M.

Statistical analysis

A Fisher's exact test was used to compare the distribution of IGHV1-2 alleles between dose groups (Fig. 1d). For alleles *02 and *04, the distribution of the ratios of unique HCDR3 counts to mRNA counts (Fig. 1h) and the ratios of HCDR3 frequency to mRNA frequency (Fig. 1j) were compared using a Wilcoxon rank sum exact test. Estimates and 95% confidence intervals (CIs) for both genotype-specific effects and the difference between the *02 and *04 per-allele effect were computed using the *lincom* function in R based on the associated linear combinations of the *02 and *04 coefficients (Fig. 2 and Supplementary Table 8). Ratio estimates and 95% CI for the relative usage of *02 and *04 from the Allele model were computed using the delta method⁴⁸ truncating the lower bound at zero (Fig. 3a and Supplementary Table 9). The 95% CI for the mean ratios of *02 to *04 mRNA expression, unique HCDR3 frequency, and BCR assignments among heterozygous vaccine recipients were computed using a *t*-distribution (Fig. 3b–d and Supplementary Table 11). The associated *P*-values for these ratios were computed using a *t*-test of the null hypothesis that the ratio is equal to one (Fig. 3d and Supplementary Table 11). The 95% CI and *P*-value for the ratio of means between homozygous *02 and homozygous *04 vaccine recipients homozygous were computed based on 10,000 bootstrap samples (Fig. 3b, c). The 95% CI and *P*-value for per-allele differences in mean mRNA expression between homozygous and heterozygous participants were computed using a *t*-test under the null hypothesis that the difference was zero (Supplementary Table 3). Comparisons of post-vaccination VRC01-class B cell frequencies between pairs of genotypes were computed using a Wilcoxon rank sum test (Supplementary Table 4). Regarding the analysis of affinity differences between populations of iGL antibodies in Fig. 5b, c, we observed an association of iGL affinity with participant ID, hence we concluded that applying tests that assume independence of all affinities would be inappropriate. To analyze the difference in mean affinity between *02 and *04 iGL Abs from Leggat et al. (Fig. 5b), we used a linear mixed effects model (LME) with fixed effects for the affinity for each allele, and a random intercept to account for within-participant correlations. To analyze the affinity difference between original *02 iGLs and their matched R66W (*05) variants (Fig. 5c), we used an LME with a fixed effect for the difference and a random intercept to account for within-participant correlations. LMEs were fit and *p*-values were evaluated using Satterthwaite's degrees of freedom method using the lmerTest package in R⁴⁹. The R language and tidyverse R packages were used for graphical and statistical analysis^{50,51}. Graphpad Prism was also used for Fig. 5.

Reporting summary

Further information on research design is available in the Nature Research Reporting Summary linked to this article.

Data availability

All data are available in the main text or supplementary materials, or in the public data repository <https://github.com/SchiefLab/G001>: first release, Zenodo (2022); <https://doi.org/10.5281/zenodo.7334877>, as described in Leggat et al.⁶. Code for the statistical modeling analysis is available in the public data repository https://github.com/SchiefLab/G001_IGHV1_2_Alleles: release v2 Zenodo (2024); <https://zenodo.org/records/10656108>.

Code availability

Code is available at the Sequencing Analysis and Data library for Immunoinformatics Exploration (SADIE) library, <https://github.com/jwillis0720/>

sadie. The IgDiscover22 v1.0.0 code used to generate the IGHV genotyping results is available at <https://gitlab.com/gkhlab/igdiscover22>.

Received: 25 April 2023; Accepted: 26 January 2024;

Published online: 11 March 2024

References

- Plotkin, S. A. Correlates of protection induced by vaccination. *Clin. Vaccine Immunol.* **17**, 1055–1065 (2010).
- Plotkin, S. A. Complex correlates of protection after vaccination. *Clin. Infect. Dis.* **56**, 1458–1465 (2013).
- Plotkin, S. A. Updates on immunologic correlates of vaccine-induced protection. *Vaccine* **38**, 2250–2257 (2020).
- Corey, L. et al. Two Randomized Trials of Neutralizing Antibodies to Prevent HIV-1 Acquisition. *N. Engl. J. Med.* **384**, 1003–1014 (2021).
- Gilbert, P. B. et al. Neutralization titer biomarker for antibody-mediated prevention of HIV-1 acquisition. *Nat. Med.* **28**, 1924–1932 (2022).
- Leggat, D. J. et al. Vaccination induces HIV broadly neutralizing antibody precursors in humans. *Science* **378**, eadd6502 (2022).
- Jardine, J. G. et al. HIV-1 VACCINES. Priming a broadly neutralizing antibody response to HIV-1 using a germline-targeting immunogen. *Science* **349**, 156–161 (2015).
- McGuire, A. T. et al. Engineering HIV envelope protein to activate germline B cell receptors of broadly neutralizing anti-CD4 binding site antibodies. *J. Exp. Med.* **210**, 655–663 (2013).
- Umotoy, J. et al. Rapid and focused maturation of a VRC01-Class HIV broadly neutralizing antibody lineage involves both binding and accommodation of the N276-Glycan. *Immunity* **51**, 141–154.e146 (2019).
- West, A. P. Jr, Diskin, R., Nussenzweig, M. C. & Bjorkman, P. J. Structural basis for germ-line gene usage of a potent class of antibodies targeting the CD4-binding site of HIV-1 gp120. *Proc. Natl Acad. Sci. USA* **109**, E2083–E2090 (2012).
- Zhou, T. et al. Structural basis for broad and potent neutralization of HIV-1 by antibody VRC01. *Science* **329**, 811–817 (2010).
- Zhou, T. et al. Multidonor analysis reveals structural elements, genetic determinants, and maturation pathway for HIV-1 neutralization by VRC01-class antibodies. *Immunity* **39**, 245–258 (2013).
- Yacoub, C. et al. Differences in allelic frequency and CDRH3 region limit the engagement of HIV Env immunogens by putative VRC01 neutralizing antibody precursors. *Cell Rep.* **17**, 1560–1570 (2016).
- Corcoran, M. M. et al. Production of individualized V gene databases reveals high levels of immunoglobulin genetic diversity. *Nat. Commun.* **7**, 13642 (2016).
- Lee, J. H. et al. Vaccine genetics of IGHV1-2 VRC01-class broadly neutralizing antibody precursor naive human B cells. *NPJ. Vaccines* **6**, 113 (2021).
- Gidoni, M. et al. Mosaic deletion patterns of the human antibody heavy chain gene locus shown by Bayesian haplotyping. *Nat. Commun.* **10**, 628 (2019).
- Peres, A. et al. IGHV allele similarity clustering improves genotype inference from adaptive immune receptor repertoire sequencing data. *Nucleic Acids Res.* **51**, e86 (2023).
- GitHub. yaarilab /IGHV_reference_book. https://yaarilab.github.io/IGHV_reference_book/02-G2.html (2022).
- Abbott, R. K. et al. Precursor frequency and affinity determine B cell competitive fitness in germinal centers, tested with germline-targeting HIV vaccine immunogens. *Immunity* **48**, 133–146.e136 (2018).
- Huang, D. et al. B cells expressing authentic naive human VRC01-class BCRs can be recruited to germinal centers and affinity mature in multiple independent mouse models. *Proc. Natl Acad. Sci. USA* **117**, 22920–22931 (2020).

21. Wang, X. et al. Multiplexed CRISPR/CAS9-mediated engineering of pre-clinical mouse models bearing native human B cell receptors. *EMBO. J.* **40**, e105926 (2021).
22. Burnham, K. P. & Anderson, D. R. Model selection and multimodel inference: a practical information-theoretic approach, Vo, 26, 2 edn (Springer New York, 2002).
23. Jardine, J. et al. Rational HIV immunogen design to target specific germline B cell receptors. *Science* **340**, 711–716 (2013).
24. Jardine, J. G. et al. HIV-1 broadly neutralizing antibody precursor B cells revealed by germline-targeting immunogen. *Science* **351**, 1458–1463 (2016).
25. Havenar-Daughton, C. et al. The human naive B cell repertoire contains distinct subclasses for a germline-targeting HIV-1 vaccine immunogen. *Sci. Transl. Med.* **10**, 448 (2018).
26. Kato, Y. et al. Multifaceted effects of antigen valency on B cell response composition and differentiation *In vivo*. *Immunity* **53**, 548–563.e548 (2020).
27. Steichen, J. M. et al. A generalized HIV vaccine design strategy for priming of broadly neutralizing antibody responses. *Science* **366**, 6470 (2019).
28. Tameris, M. et al. Live-attenuated mycobacterium tuberculosis vaccine MTBVAC versus BCG in adults and neonates: a randomised controlled, double-blind dose-escalation trial. *Lancet Respir. Med.* **7**, 757–770 (2019).
29. Crank, M. C. et al. Safety and immunogenicity of a rAd35-EnvA Prototype HIV-1 vaccine in combination with rAd5-EnvA in healthy adults (VRC 012). *PLoS One.* **11**, e0166393 (2016).
30. Sasso, E. H., Buckner, J. H. & Suzuki, L. A. Ethnic differences of polymorphism of an immunoglobulin VH3 gene. *J. Clin. Invest.* **96**, 1591–1600 (1995).
31. Feeney, A. J., Atkinson, M. J., Cowan, M. J., Escuro, G. & Lugo, G. A defective Vkappa A2 allele in Navajos which may play a role in increased susceptibility to haemophilus influenzae type b disease. *J. Clin. Invest.* **97**, 2277–2282 (1996).
32. Liu, L. & Lucas, A. H. IGH V3-23*01 and its allele V3-23*03 differ in their capacity to form the canonical human antibody combining site specific for the capsular polysaccharide of Haemophilus influenzae type b. *Immunogenetics* **55**, 336–338 (2003).
33. Watson, C. T. & Breden, F. The immunoglobulin heavy chain locus: genetic variation, missing data, and implications for human disease. *Genes Immun.* **13**, 363–373 (2012).
34. Throsby, M. et al. Heterosubtypic neutralizing monoclonal antibodies cross-protective against H5N1 and H1N1 recovered from human IgM + memory B cells. *PLoS One.* **3**, e3942 (2008).
35. Ekiert, D. C. et al. Antibody recognition of a highly conserved influenza virus epitope. *Science* **324**, 246–251 (2009).
36. Sui, J. et al. Structural and functional bases for broad-spectrum neutralization of avian and human influenza A viruses. *Nat. Struct. Mol. Biol.* **16**, 265–273 (2009).
37. Dreyfus, C. et al. Highly conserved protective epitopes on influenza B viruses. *Science* **337**, 1343–1348 (2012).
38. Pappas, L. et al. Rapid development of broadly influenza neutralizing antibodies through redundant mutations. *Nature* **516**, 418–422 (2014).
39. Wheatley, A. K. et al. H5N1 vaccine-elicited memory B cells are genetically constrained by the IGHV locus in the recognition of a neutralizing epitope in the hemagglutinin stem. *J. Immunol. Res.* **195**, 602–610 (2015).
40. Avnir, Y. et al. IGHV1-69 polymorphism modulates anti-influenza antibody repertoires, correlates with IGHV utilization shifts and varies by ethnicity. *Sci. Rep.* **6**, 20842 (2016).
41. Sok, D. & Burton, D. R. Recent progress in broadly neutralizing antibodies to HIV. *Nat. Immunol.* **19**, 1179–1188 (2018).
42. Vazquez Bernat, N. et al. High-quality library preparation for NGS-based immunoglobulin germline gene inference and repertoire expression analysis. *Front. Immunol.* **10**, 660 (2019).
43. Narang, S., Kaduk, M., Chernyshev, M., Karlsson Hedestam, G. B. & Corcoran, M. M. Adaptive immune receptor genotyping using the corecount program. *Front. Immunol.* **14**, 1125884 (2023).
44. Dunn, P. K. & Smyth, G. K. *Generalized Linear Models With Examples in: R* 1st edn (Springer-Verlag, New York Inc., 2018).
45. McCullagh, P. & Nelder, J. A. *Generalized Linear Models* 2nd edn (Chapman & Hall/CRC, 1998).
46. Ye, J., Ma, N., Madden, T. L. & Ostell, J. M. IgBLAST: an immunoglobulin variable domain sequence analysis tool. *Nucleic Acids Res.* **41**, W34–W40 (2013).
47. Breden, F. et al. Reproducibility and reuse of adaptive immune receptor repertoire data. *Front. Immunol.* **8**, 1418 (2017).
48. Fox, J. *Applied Regression Analysis and Generalized linear models* 3rd edn (SAGE, 2016).
49. Kuznetsova, A., Brockhoff, P. B. & Christensen, R. H. B. ImerTest package: tests in linear mixed effects models. *J. Stat. Softw.* **82**, 1–26 (2017).
50. Wickham, H. et al. Welcome to the tidyverse. *J. Open Source Softw.* <https://doi.org/10.21105/joss.01686> (2019).
51. R Core Team. *R: A Language and Environment for Statistical Computing.* <https://www.R-project.org/> (2019).

Acknowledgements

We thank Pervin Anklesaria, Nina Russell, and Emilio Emini for discussions and trial planning; Jeong Hyun Lee for comments on the manuscript; Olayinka Fagbayi and Amelia Mosley of IAVI for project management at the IAVI NAC at Scripps. This work was supported by the Bill and Melinda Gates Foundation Collaboration for AIDS Vaccine Discovery (CCVIMC INV-007371 to R.A.K., A.B.M., and M.J.M.; VISC INV-008017 and INV-032929 to A.C.D.; VxPDC INV-008352 and INV-007375 to IAVI; and NAC INV-007522 and INV-008813 to W.R.S.), IAVI (including IAVI 167627819 to M.J.M. and other support to W.R.S.), the IAVI Neutralizing Antibody Center (NAC) to W.R.S., National Institute of Allergy and Infectious Diseases (NIAID) P01 AI094419 (HIVRAD Optimizing HIV immunogen-BCR interactions for vaccine development”) (to W.R.S.), UM1 AI100663 (Scripps Center for HIV/AIDS Vaccine Immunology and Immunogen Discovery) and UM1 AI144462 (Scripps Consortium for HIV/AIDS Vaccine Development) (to W.R.S. and M.J.M.); and UM1AI069481 (Seattle-Lausanne CTU), U19AI128914 (HIPC), and UM1AI068618 (HVTN LC) to M.J.M.; and by the Ragon Institute of MGH, MIT, and Harvard (to W.R.S.).

Author contributions

W.J.F., M.M.C., J.R.W., A.C.D., G.B.K.H. and W.R.S. designed the study. C.A.C., D.L.V.B., and W.R.S. designed SPR studies. O.Ka. and A.L. performed SPR studies. T.-M.M. produced antibodies for SPR. D.J.L., K.W.C., M.J.M., R.A.K., A.C., A.B.M., L.B.-F., A.S., J.R.P., R.E.W., A.S., J.B., A.M.R., W.H., D.R.A., S.M., F.R., A.L., V.P., D.S.L., A.T., D.M.B., M.R., J.M., O.K., N.K., J.B., D.D., planned, supervised, or carried out clinical trial activities or B cell sorting and sequencing assays or data organization leading to the data analyzed here. M.M.C and G.B.K.H. provided VH1-2 genotype analyses and quantification of mRNA and HCDR3 frequencies. J.R.W. provided VH1-2 allele inferences for post-vaccination BCRs. W.J.F., O.H., and A.C.D. performed statistical modeling and analyses. A.C.D., M.M.C, G.B.K.H., and W.R.S. wrote the main text and supplementary materials. A.C.D. and W.R.S. created figures and tables. A.C.D., M.M.C., and W.J.F. contributed equally to this work.

Funding

Open access funding provided by Karolinska Institute.

Competing interests

W.R.S. and S.M. are inventors on patents filed relating to the eOD-GT8 60mer immunogen in this manuscript. M.M.C and G.B.K.H. are founders of ImmuneDiscover Sweden AB. W.R.S. is an employee of Moderna, Inc., A.C. is an employee of Nykode Therapeutics, and A.B.M. is an employee of Sanofi. All other authors declare no competing interests.

Additional information

Supplementary information The online version contains supplementary material available at <https://doi.org/10.1038/s41541-024-00811-5>.

Correspondence and requests for materials should be addressed to Allan C. deCamp, Gunilla B. Karlsson Hedestam or William R. Schief.

Reprints and permissions information is available at <http://www.nature.com/reprints>

Publisher's note Springer Nature remains neutral with regard to jurisdictional claims in published maps and institutional affiliations.

Open Access This article is licensed under a Creative Commons Attribution 4.0 International License, which permits use, sharing, adaptation, distribution and reproduction in any medium or format, as long as you give appropriate credit to the original author(s) and the source, provide a link to the Creative Commons licence, and indicate if changes were made. The images or other third party material in this article are included in the article's Creative Commons licence, unless indicated otherwise in a credit line to the material. If material is not included in the article's Creative Commons licence and your intended use is not permitted by statutory regulation or exceeds the permitted use, you will need to obtain permission directly from the copyright holder. To view a copy of this licence, visit <http://creativecommons.org/licenses/by/4.0/>.

© The Author(s) 2024